

行政院國家科學委員會專題研究計畫成果報告

陡坡渠道潰壩流況之水理分析

Hydraulic Analysis of Dam-Break Flow in Steep Channel

計畫編號：NSC 89-2211-E-002-141

執行期限：89年8月1日至90年7月31日

計畫主持人：許銘熙 國立臺灣大學農業工程學系教授

計畫參與人員：鄧慰先 國立臺灣大學水工試驗所博士後研究

陳春宏 國立臺灣大學農業工程學系博士

蘇騰鎰 國立臺灣大學農業工程學系博士研究生

中文摘要

本文主要在以數值方法模擬斜坡渠道上潰壩流場之波傳。為掌握自由水面不規則移動邊界之變化，採用動格網方式配合邊界閉合座標法，並將不規則物理平面座標轉換成規則之計算平面上進行求解。對於二維動量及連續方程之控制方程式之求解，採用非交錯格網系統以有限差分法離散控制方程式，並以交替拉格蘭吉-尤拉運動描述法來模擬自由水面之波傳現象。本文利用潰壩流場之實驗資料作為模式之驗證，進而模擬各渠床坡度之潰壩流場。

關鍵詞：波傳，邊界閉合座標，自由水面，潰壩。

Abstract

The wave propagation of dam break flows in a sloping smooth channel was simulated by numerical model in this paper. In order to obtain movable boundaries on the free surface, the techniques of the moving grids and boundary-fitted coordinate system presented by Thompson are adopted. The solutions were obtained by transforming the irregular physical domain into regular computational domain. The governing equations of the two-dimensional momentum and continuity equations were solved simultaneously by using the finite difference scheme on nonstaggered grids. The arbitrary Lagrangian - Eulerian (ALE) kinematic description was applied in the procedure of calculation. The numerical

model was verified by experimental data of wave propagation due to a dam failure. As a result, the model was used to simulate and analyse the wave propagation of dam break in different sloping channel

Keywords: wave propagation, boundary fitted coordinate, free surface, dam break

一、緣由與目的

潰壩流場在水利工程上是一個重要且實際之研究問題，包括潰壩後最大水深、最大流量及水流到達某一位置之時間等，此常為水利工程師在設計規劃時重要參考，故對於潰壩流場的掌握相對的重要。然而一般潰壩理論常僅適用於渠底為水平之渠道，對於一般壩體興建於河道之上游，且河道坡度較陡之情況並不適用，因此對斜坡上潰壩流場之模擬有其必要性。本計畫已完成陡坡潰壩水理及影響陡坡潰壩水理參數之理論分析，建立陡坡潰壩垂直二維水理數值模式，並獲得陡坡潰壩垂直二維流場及壓力分布之模擬結果。本計畫研究成果已經發表於國內外相關研究期刊。

過去對於具有移動邊界之潰壩問題以有數種模式被提出，其以一維模式較常被使用，其中對於水平渠道方面解析解有 Stoker (1957) 及 Dressler (1952) 提出，數值解則有 Chen and Armbruster (1980), Bellas and Sakkas (1987), Yung et al, (1993) 及許 (1995) 等。對於斜坡渠道上之潰壩流場方面解析解有 Hunt (1987) 提出，一維數值計算則有 Sakkas and Strelkoff (1976), and

Aguirre-pe, Plachco and Quisca (1995) and Jin and Fread (1997)等進行模擬。而在斜坡渠道上之二維潰壩流場模擬方面則甚少學者提出。在實驗部份 Martin and Moyce (1952), Lauber 等(1998)曾針對水平渠道之潰壩流場進行試驗, 美國陸軍工程兵團(1960,1961)、Lauber 等(1998)曾針對斜坡渠道之潰壩流場進行試驗。

對於二維水流之計算常利用 Navier - Stokes 方程式來計算, 以數值方法解 Navier - Stokes 方程式來模擬含自由水面的問題, 常依其座標系統描述方式可分兩種。一為尤拉格點描述法(Eulerian grid), 二為拉格蘭吉格點(Lagrangian grid)描述法; 在尤拉座標系統為基礎的計算方法中, 以 Harlow 和 Welch(1965) 利用有限差分法發展的 MAC(Marker and Cell)最常被使用; 對於拉格蘭吉描述法, 其能直接由格網的形狀變化求出自由水面或界面的形狀, 且自由水面的邊界較易處理, 並可用於任意曲形的固體邊界, 但其最大的缺點在於無法承受流體過度的扭曲。有些學者利用結合拉格蘭吉和尤拉格點之方法, 稱為 Arbitrary Lagrangian - Eulerian method (簡稱 ALE), 其為避免邊界移動造成過度變形, 乃引進一網格速度來調整格網, 此一網格速度於演算過程中並入動量方程式之對流項中, 以使數值更為穩定且減少網格過度變形, 其詳細說明見許(2000, 2001)。

二、控制方程式

若水流沿渠寬之側向流況變化甚小, 假設水平渠底, 並且忽略流體表面受風剪應力與地球自轉等效應, 及考慮非紊流況則垂直平面二維連續方程式與運動方程可寫為如下:

$$\frac{\partial U}{\partial x} + \frac{\partial W}{\partial z} = 0 \quad (1)$$

$$\frac{\partial U}{\partial t} + U \frac{\partial U}{\partial x} + W \frac{\partial U}{\partial z} = -\frac{\partial \phi}{\partial x} + \nu \left(\frac{\partial^2 U}{\partial x^2} + \frac{\partial^2 U}{\partial z^2} \right) \quad (2)$$

$$\frac{\partial W}{\partial t} + U \frac{\partial W}{\partial x} + W \frac{\partial W}{\partial z} = -\frac{\partial \phi}{\partial z} + \nu \left(\frac{\partial^2 W}{\partial x^2} + \frac{\partial^2 W}{\partial z^2} \right) - g \quad (3)$$

其中, t : 為時間座標; x : 為橫向座標(水平方向); z : 為縱向座標(垂直方向); ν : 流體運動黏滯係數(kinematic viscosity);

ϕ : 壓力比值, 即壓力 P 對流體密度之比(即 $\phi = P/\rho$); $\frac{\partial}{\partial x}, \frac{\partial}{\partial z}$: 為沿 x 或 z 方向之偏微分運算子; U : 沿 x 方向之水平流速; W : 沿 z 方向之垂直流速; g : 重力加速度; (1)(2) 及(3)式分別表示水流之連續方程式、 x 及 z 方向之運動方程式。

在邊界條件方面, 本文所討論之自由水面問題, 其邊界條件可分成固定邊界條件及自由水面邊界條件。固定邊界係指不可穿透之邊界, 即在邊界處沒有流體通量通過, 本研究對於河道底床採用滑動邊界條件, 依據 Abbrtt(1978)與 Anderson (1984)認為於邊牆之邊界條件上之合速度應上切於邊壁。Jimenez(1988)曾提出虛擬邊界法, 該法以一反射程序應用於邊牆之邊界條件。若邊壁與 x 軸相交角度 θ , 而在假設點之合速度與 x 軸相交角度 α , 則本文在假設點之速度分量 u_f 和 v_f 分別為

$$u_f = V \cos(\theta - \alpha) \quad (4)$$

$$v_f = V \sin(\theta - \alpha)$$

式中 V 為流場內之點或其相對假設點之合速度。

三、邊界閉合座標轉換

以本研究採用 Thompson(1982)之微分方程法進行格網之建立, 使物理平面(x, z 座標)變換到計算平面(ξ, η)。計算過程中, 控制方程式亦須由從物理平面(t, x, z)轉換至計算平面(t, ξ, η), 在使用鍊微法則(chain rule)處理各偏微分項後, 可將式(1)、(2)、(3)轉換為:

連續方程式

$$U_\xi \xi_x + W_\xi \xi_z + U_\eta \eta_x + W_\eta \eta_z = 0 \quad (5)$$

運動方程式

$$U_t + (\xi_x \bar{U} + \xi_z \bar{W}) U_\xi + (\eta_x \bar{U} + \eta_z \bar{W}) U_\eta = -[\xi_x \phi_\xi + \eta_x \phi_\eta] + \nu(\text{vis}_x) \quad (6)$$

$$W_t + (\xi_x \bar{W} + \xi_z \bar{W}) W_\xi + (\eta_x \bar{W} + \eta_z \bar{W}) W_\eta = -[\xi_z \phi_\xi + \eta_z \phi_\eta] + \nu(\text{vis}_z) - g \quad (7)$$

式中, $\bar{U} = U - x_t$; $\bar{W} = W - z_t$;

$$\text{vis}_x = \left(\frac{\alpha}{J} U \right)_{\xi\xi} + \left(\frac{\beta}{J} U \right)_{\xi\eta} + \left(\frac{\gamma}{J} U \right)_{\eta\eta} - \left(\frac{\nabla^2 \xi}{J} U \right)_\xi - \left(\frac{\nabla^2 \eta}{J} U \right)_\eta$$

$$\text{vis}_z = \left(\frac{\alpha}{J} W \right)_{\xi\xi} + \left(\frac{\beta}{J} W \right)_{\xi\eta} + \left(\frac{\gamma}{J} W \right)_{\eta\eta} - \left(\frac{\nabla^2 \xi}{J} W \right)_\xi - \left(\frac{\nabla^2 \eta}{J} W \right)_\eta$$

其中, $\alpha = \xi_x^2 + \xi_z^2$; $\beta = 2(\xi_x \eta_x + \xi_z \eta_z)$;

$\gamma = \eta_x^2 + \eta_z^2$; $\xi_x = z_\eta / J$, $\eta_x = -z_\xi / J$, $\xi_z = -x_\eta / J$,
 $\eta_z = x_\xi / J$, $J = \xi_x \eta_z - \xi_z \eta_x$; $\nabla^2 \xi = \xi_{xx} + \xi_{zz}$;
 $\nabla^2 \eta = \eta_{xx} + \eta_{zz}$; x_i 表水平方向之網格移動速度,
 z_i 表垂直方向之網格移動速度。

四、數值方法

本文以顯式差分法離散時變項，其數值方法則為條件穩定，然其代數方程組系統則為線性且較為簡單，其所需電腦記憶空間較小，且容易求解。首先將式(6)及(7)分別對 x 與 z 偏微後相加，並使用後項差分對時間導數項 U_i 及 W_i 進行離散，可得

$$\alpha \phi_{\xi\xi}^{n+1} + \beta \phi_{\xi\eta}^{n+1} + \gamma \phi_{\eta\eta}^{n+1} = \bar{A} \xi \xi_x + \bar{A} \eta \eta_x + \bar{B} \xi \xi_z + \bar{B} \eta \eta_z \quad (8)$$

其中

$$\bar{A} = U^n - \Delta t [(\xi_x \bar{U}^n + \xi_z \bar{W}^n) U_\xi^n + (\eta_x \bar{U}^n + \eta_z \bar{W}^n) U_\eta^n - v(\text{vis}x)] \quad (9)$$

$$\bar{B} = W^n - \Delta t [(\xi_x \bar{U}^n + \xi_z \bar{W}^n) W_\xi^n + (\eta_x \bar{U}^n + \eta_z \bar{W}^n) W_\eta^n - v(\text{vis}z) + g] \quad (10)$$

式中 \bar{A}, \bar{B} 為計算過程中之流速其非真實之流速，僅為計算過程中之中繼值。本研究係利用式(8)依疊代法求解壓力比值 ϕ^{n+1} 。式(6)及式(7)可將 $n+1$ 時階之流速 U^{n+1}, W^{n+1} 表示為

$$U^{n+1} = -\Delta t (\phi_\xi^{n+1} \xi_x + \phi_\eta^{n+1} \eta_x) + \bar{A} \quad (11)$$

$$W^{n+1} = -\Delta t (\phi_\xi^{n+1} \xi_z + \phi_\eta^{n+1} \eta_z) + \bar{B} \quad (12)$$

將式(8)計算之 ϕ^{n+1} 值，代入式(11)及式(12)中，計算流速 U^{n+1}, W^{n+1} 值。但疊代過程中所得之 U^{n+1} 及 W^{n+1} 未必滿足連續方程式，利用下式判斷其是否符合連續方程並加以修正。

$$D^k = (U_\xi^{n+1,(k)} \xi_x + U_\eta^{n+1,(k)} \eta_x + W_\xi^{n+1,(k)} \xi_z + W_\eta^{n+1,(k)} \eta_z) \quad (13)$$

D^k 即為流場格點於 $n+1$ 時階疊代次數 k 時流速之連續方程誤差值。本文採用 D^k 作為壓力比值 ϕ 之修正即

$$\phi^{n+1,k+1} = \phi^{n+1,k} - C \times D^k \quad (14)$$

其中 C 為鬆弛因子，若連續方程式平均誤差值 \bar{D} 大於容許度，則將式(14)所得之壓力比值 ϕ^{n+1} 代入式(11)與(12)中求出流速，再將求得之流速代入式(13)中，若連續方程平均誤差值仍大於容許度則代入式(14)修正 ϕ^{n+1} ，如此反覆上述之步驟，直至

平均誤差值小於容許度為止。本研究鬆弛因子 C 採 $1.8m^2/sec \cdot \bar{D}$ 大於容許度採 10^{-4} 。

五、動格網的建立

求解非定常流體動力學時，在物理平面之格網隨時間改變而產生變化，故在數值計算上必須隨時間的變化而建立新的格網。以下就針對本研究之動格網建立加以說明：

設從 t 時刻開始計算，已知物理平面內求解域邊界各格點 t 時刻之位置 $(x', z')_s$ 和各格點的移動速度 $(U', W')_s$ ，下標 s 表邊界。從已知的 $(x', z')_s$ ，利用邊界閉合座標方法作出求解域內的曲線格網，以確定各格網點的位置 (x', z') 。從已知的 $(U', W')_s$ 和 $(x', z')_s$ 可以算出 Δt 時間後新的求解域之估算邊界點位置 $(Ex, Ez)_s^{t+\Delta t}$ 。其為

$$\begin{pmatrix} Ex \\ Ez \end{pmatrix}_s^{t+\Delta t} = \begin{pmatrix} x \\ z \end{pmatrix}_s + \begin{pmatrix} U \\ W \end{pmatrix}_s \Delta t \quad (15)$$

由上式計算之邊界其網格大小不一，為避免求出的邊界位置在建立內部格網時，造成內部格網過度扭曲，乃將邊界網格重新劃分成均勻網格。本研究利用 ALE 方法重新定義求解域邊界位置，首先選定邊界在 x 或 z 方向上投影較長者進行等間距之網格分割，其網格點之座標可利用已均勻劃分之 x 或 z 軸點座標與估算邊界點位置 $(Ex, Ez)_s^{t+\Delta t}$ 間線性內差方式求得。如圖 1 所示， x 方向為自由水面投影在座標軸上較長者，其在時間 $t + \Delta t$ 時等劃分之 x 方向新座標為 $x_{\eta_i}^{t+\Delta t}$ ，其 z 方向之座標 $z_{\xi_i}^{t+\Delta t}$ 可由 $x_{\eta_i}^{t+\Delta t}$ 與估算邊界點位置 $(Ex, Ez)_s^{t+\Delta t}$ 利用線性內差求得。而其自由水面上格網點之格網移動速度計算如下

$$\begin{pmatrix} x_i \\ z_i \end{pmatrix}_{\eta_i} = \begin{pmatrix} x^{t+\Delta t} - x^t \\ z^{t+\Delta t} - z^t \end{pmatrix}_{\eta_i} / \Delta t \quad (16)$$

新的物理平面之內部網格點利用邊界之網格點配合 Poisson 方程求得 $(x, z)_i^{t+\Delta t}$ ，而其格網移動速度為 $x_i = (x_i^{t+\Delta t} - x_i^t) / \Delta t$ ， $z_i = (z_i^{t+\Delta t} - z_i^t) / \Delta t$ 。

六、結果討論

有關潰壩流場分析主要在於了解潰壩後其對下游河道之影響，包括最大流量，

最大水深及洪水到達時間等。本文乃藉由數值模式模擬各種坡度下之潰壩流場，並以Lauber and Hager(1998)之試驗資料作驗證，以確定本模式之適用性。進而針對潰壩後波前移動、最大水深、最大流量等之估算，提供一簡易圖或方程式，以供估算各坡度下潰壩水理之參考。圖2為一有限長度水庫於斜坡渠道上之示意圖。

過去有關斜坡渠道上潰壩之解析解有Hunt(1987)其假設非黏性水流及斜坡角度 θ (以徑度表示)趨近渠道坡度 S_0 ，適用於微小坡度渠道，利用特性線法求解一維之迪聖凡納氏方程式(de Saint Venant Equation)。

現若考慮於壩址處水深 $h_0=1\text{m}$ ，初始下游渠道河床為乾床，即水深為零。假設河床均為平滑無剪力作用，分別就渠道坡度為0.01、0.1、0.2及0.5進行潰壩模擬，數值計算時格網數為 31×15 ，由於潰壩流場之流速甚大，且潰壩流場水體變化易造成垂向網格間距變小，為避免數值計算時造成數值不穩定之現象，時間間距 $\Delta t = 5 \times 10^{-4}$ 秒。模擬結果與Hunt(1987)假設不考慮流體黏性、 $\theta \approx S_0$ 之解析解及Lauber and Hager(1998)平滑渠道潰壩試驗之無因次資料進行比較如圖3所示，由圖中很明顯發現解析解因忽略黏性效應且假設渠道坡度 $\theta \approx S_0$ ，當應用於大坡度渠道上之潰壩，其與數值解及實驗資料比較相差甚大，在同一時間下其移動距離亦較數值解及實驗資料大的甚多。而數值計算結果在坡度 $S_0=0.1$ 及 $S_0=0.5$ 與實驗資料甚為接近，顯示本模式之適用性。故圖3可供估算各坡度下潰壩到達某一位置之時間。

圖4為潰壩後下游河道於不同位置時之最大水深，將最大水深沿渠道斜坡方向移動之距離乘以河道坡度表示後，可以發現各坡度之潰壩於下游各位置之最大水深相當接近，圖中實線為 $S_0=0.1$ 之實驗資料其與數值模擬結果 $S_0=0.1$ 之曲線亦甚為接近，惟在水深較低時具有較大誤差，此可能由於本模式在底床邊界採用滑動邊界所致。在水深較低時其受底床剪力影響較大，以致產生較大之誤差。另對於 $S_0=0.5$ 之實驗資料，由於Lauber and Hager(1998)之試驗結果因瞬間潰壩時受壩體移動之干

擾，以致在不同位置之水面歷線具有多峰現象，故本文以其歸納之最大水深與壩址下游位置之關係式作比較，其關係式如下：

$$\frac{z_m}{h_0} = \frac{4}{9}(1 + \bar{X}^{-1})^{-5/4} \quad (17)$$

其中 z_m 為在壩址下游 x 距離處之最大水深， $\bar{X} = L_b(h_0 x^{-2})^{-1/3}$ ， L_b 之定義如圖2所示。將方程式點繪如圖4中之粗實線，其結果與本模式計算之結果甚為接近，顯示本模式針對不同坡度渠道潰壩模擬具有一定之準確性。若將數值計算各坡度之壩址下游潰壩最大水深取迴歸後可得

$$z_m/h_0 = 0.195(\bar{x}S_0/h_0)^{-0.339} \quad (18)$$

此方程式可提供估算各種坡度在潰壩後壩址下游位置最大水深，上述之方程式因接近壩址處其水深趨於無窮大，其適用於 $\bar{x}S_0$ 大於0.1之情形。

圖5為渠道坡度0.1時在壩址下游 $\bar{x}/h_0=1$ 及4處水深歷線之數值模式與實測資料比較，由圖中可知在水波到達 $\bar{x}/h_0=1$ 及4時間方面數值模式與實驗資料甚為接近，而發生最大水深之時間數值模式較實驗資料提前，此部份本模式尚無法有效之掌握，但其壩址下游位置發生之最大水位數值模式與實驗資料甚為接近，故本文對不同渠床坡度潰壩時，其壩址下游位置發生最大水深時間暫不提供估算。圖中數值模式與實驗資料發生最大誤差在潰壩後洪水之退水段部份，在水深 \bar{z}/h_0 大於0.15時數值模擬與實驗資料甚為接近，而水深 \bar{z}/h_0 小於0.15時數值模擬結果明顯較實驗資料為快，此乃因潰壩後洪水之退水段其水深較淺，受底床剪力之作用甚大，由於本模式尚未考慮底床剪力之影響，故數值模式中洪水之退水時間較實測資料為快，但洪水之退水段其水深較淺，其對河道危害較小，故其重要性亦不高。

七、結論

本模式利用滑動邊界於斜坡渠道上，來模擬各種坡度下潰壩流場，由於本研究之模式固定邊界採滑動邊界條件對於邊界剪力作用較小之流場模擬具有較佳之模擬成果，經試驗資料比較顯示在高水位時本模式具有相當之精確度，而在低水位時，

因其流場受底床剪力影響較大，由於本模式因採用滑動邊界，無法反應底床之阻力，故對於低水位時模擬結果與試驗資料具有較大誤差，但以工程設計觀點，對於潰壩後壩址下游產生最大流量、各位置之最大水深及波前運動等較為重要，此部份本模式已有效捕捉，且提供一簡易之圖或方程式以供估算。本計畫研究成果已經發表於國內外相關研究期刊。

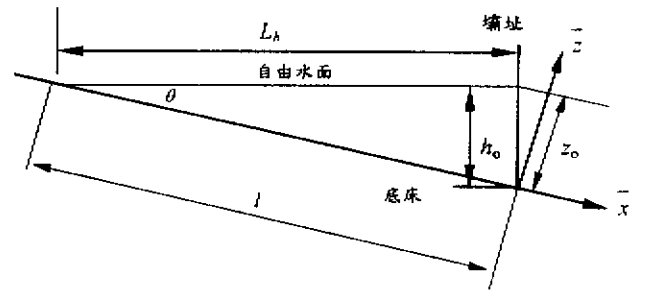


圖 2 有限長度潰壩初始示意圖

八、參考文獻

1. Stoker, J. J., *Water wave*, John Wiley & sons, Inc., pp. 333-341 (1957).
2. 許銘熙, 「自由水面之二維垂直水理模式」, 行政院國科會專題研究計畫報告, 台北 (1995)。
3. Hunt, B., "An inviscid dam-break solution," *Journal of Hydraulic Research*, Vol. 25, No. 3, pp. 313-327 (1987).
4. Lauber, G. and Hager, W. H., "Experiments to dambreak wave: Sloping channel," *Journal of Hydraulic Research*, Vol. 36, No. 5, pp. 761-773 (1998).
5. 許銘熙, 陳春宏, 2001.6, 平滑斜坡渠道之二維潰壩分析, 中國土木水利工程學刊, 第 13 卷第 2 期, 405-414 (2000)。
6. Hsu, M.H., Chun-Hung Chen, and Teng, W.H., "An Arbitrary Lagrangian - Eulerian Finite Difference Method for Computations of Free Surface Flows," *Journal of Hydraulic Research*, 2001. (in press, SCI)
7. Thompson, J. F., Warsi, Z. U. A. and Mastin, C.W., "Boundary-fitted coordinate system for numerical solution of partial differential equation - A review," *Journal of Computational Physics*, Vol. 47, pp.1-108 (1982).

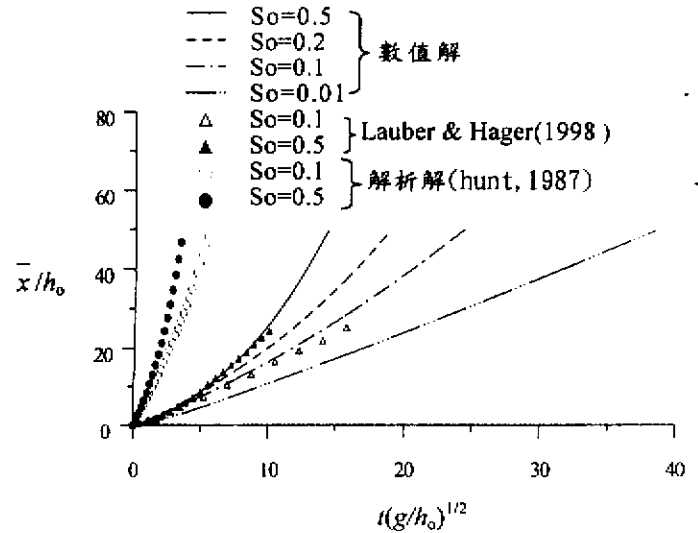


圖 3 潰壩波前移動之數值模式、實驗資料及解析解比較

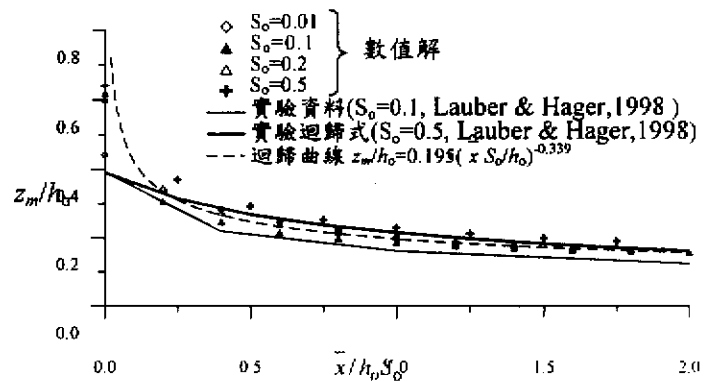


圖 4 潰壩後下游各位置之最大水深

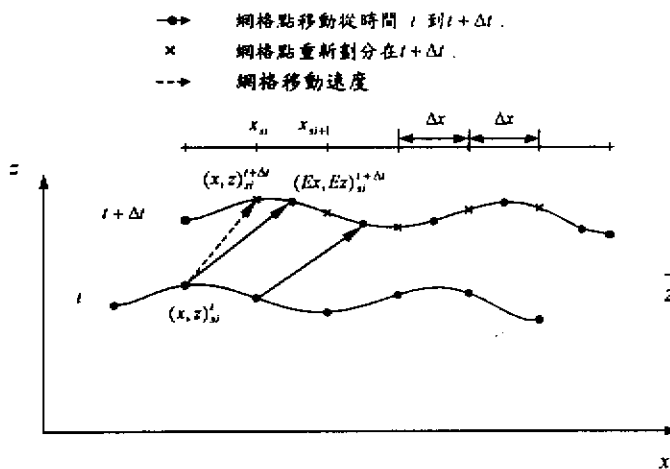


圖 1 動格網移動及網格重新劃分示意圖

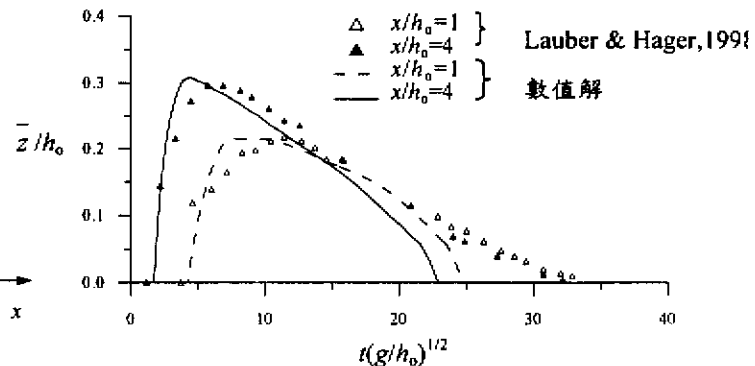


圖 5 渠道坡度 \$S_0=0.1\$ 潰壩後之水深歷線

行政院國家科學委員會補助國內專家學人出席國際學術會議報告

90年6月25日

| | | | |
|--|---|---------------|--|
| 報 告 人 姓 名 | 許 銘 熙 | 服務機構 及 職 稱 | 台灣大學農業工程學系 教授兼主任 |
| 會 議 時間 地點 | 90年6月11日~6月15日 加拿大 Edmonton | 本會核定 補助文號 | 陡坡渠道潰壩流況之水理分析 NSC 89-2211-E-002-141 |
| 會 議 名 稱 | (中文)：第三屆波浪現象國際研討會 (英文)：Wave Phenomena III | | |
| 發表論文題目 | (中文)：河口潮汐入侵峰之探討 (英文)：Investigation of the Tidal Intrusion Front in Estuary | | |
| <p>一、參加會議經過</p> <p>第三屆波浪現象國際研討會(Wave Phenomena III: Waves in Fluids from the Microscopic to the Planetary Scale)於2001年6月11日至15日在加拿大Edmonton市區之Alberta大學舉行，本會第一屆與第二屆分別於1983年與1992年舉行，每間隔九年舉行一次，今年是屬第三屆。本次會議之主要目的是集合從事波浪方面研究的學者、專家、工程師等齊聚一堂，進行廣泛的討論與意見交換。本會的主辦單位為亞伯特大學與太平洋數學科學及應用數學研究所共同籌辦，參加者主要來自於加拿大、美國、英國、日本、中國大陸、台灣、香港、德國等國，與會人數約200餘人，發表之大會邀請論文23篇；參與投稿論文計有100篇；合計發表文章123篇，並出版議程及論文摘要各一冊。</p> <p>研討會開幕式由當地組織委員會主席Dr. Andrew B.G. Bush先生主持，隨即由大會邀請之講者發表論文，由上午8:30至下午2:50共有六篇文章於全體與會者出席的會議廳舉行，於下午3:30以後共分5個小型會議分組發表論文。由於有關波浪現象的研究領域甚為廣泛包括數學應用、解析及數值模式發展等，所以大會並沒有針對特定主題予以分類。</p> <p>二、與會心得</p> <p>分組討論中，我的論文被大會安排在六月十四日(星期四)下午，分組討論的主持人為Dr. Andrew B. G. Bush先生，我所發表之論文題目為「Investigation of the Tidal Intrusion Front in Estuary」。同一分組發表的有香港科技大學學者發表「Synchronous Coupling of a Wave Propagation Model and a 3D Tidal Model」與我們研究領域較相近，主要討論結合波浪傳遞模式與三維水理模式用以預測波浪及海流間的交互作用。波浪模式是以波浪作用守衡程式，並考慮反射與折射波浪的影響，三維水理模式是結合波浪模式包括波-流底部邊界層模式及垂直剪力黏滯係數。此波浪與海浪模式應用於南中國海的Pearl River河口，與實測資料比較結果大致不錯。台灣的波浪模式大多引用國外模式如WAM (Wave Model)、WAVEWATCH 波浪與潮流模式、SWAMP 模式、荷蘭Delft</p> | | | |

大學主導發展之波浪模式等，結合波浪與海流作用的三維數值模式是值得台灣學者與研究機構的引用與發展。

三、考察參觀活動(無是項活動者省略)

四、建議

(1)海洋與河口研究已有相當歷史，國內對海洋研究往往投入很多研究經費（包括有研究船及高科技的監測儀器）用於觀測資料的取得，對於數值模式發展也是近幾年的事，冀望觀測資料之蒐集與模式之分析能相輔相成，相互印證。

(2)國內對於海洋與河口模式的發展應該投入更多的人才，如此才能在國際學術地位上更有所精進。

五、攜回資料名稱及內容

本次參加波浪現象國際研討會攜回資料包括論文摘要一本。

INVESTIGATION OF THE TIDAL INTRUSION FRONT IN ESTUARY

Wen-Cheng Liu,¹ Ming-Hsi Hsu² and Albert Y. Kuo³

¹ Hydrotech Research Institute, National Taiwan University, Taipei 10617, Taiwan.

² Department of Agricultural Engineering and Hydrotech Research Institute, National Taiwan University, Taipei 10617, Taiwan.

³ School of Marine Science / Virginia Institute of Marine Science,
The College of William and Mary, Gloucester Point, Virginia 23062, U.S.A

ABSTRACT

When fresh water discharges into an estuary or directly into the sea, a frontal system may be formed with relatively fresh water overlaying the saline water. The front can be measured part, at the surface, for the interface between these layers. The typical way to describe the stratification conditions present in an estuary is by using Froude number. Another way to study time-varying conditions in tidal estuaries is by means of gravity (or density) currents. This theory has usually been employed in relation to a wedge of heavy fluid intruding into a lighter fluid. However, opposite situations, such as those in which river water propagates into estuarine or seawater, also correspond to a gravity current condition. A laterally averaged two-dimensional model is applied to the Tanshui River estuary and is used to calculate the hydrodynamic conditions which are taken as basic data. A tidal Froude number, which is the natural form, is employed. Instantaneous values for this parameter, which takes into account the existence of significant tidal currents in the lower layer, are calculated for the Tanshui River estuary in order to characterize the evolution of their stratification. Additionally, hydrodynamic data of an estuary are employed to verify how well the gravity current theory is satisfied. It is shown that gravity current theory approximately holds under tow-layers condition in the regions near to the head of the front and developed processes.

Keywords: Tidal intrusion front, Froude number, Gravity current, Estuarine stratification, Tanshui River estuary.

INTRODUCTION

In recent years, the widespread occurrence of fronts in estuarine and coastal waters has been examined and their potentially key role in determining characteristics of circulation and mixing in a variety of physical settings has been established. Implications for a range of ecological and environmental questions have provided ample motivation for research dealing with various aspects of fronts.

Fronts associated with estuaries are often transient and local phenomena, related to particular basin features and/or to particular part of the tidal cycles. Various names have been assigned to different types of fronts according to their features or to the mechanisms responsible for their generation. Plume fronts form and evolve near the mouths of some estuaries during ebb tide, when the less-dense estuaries discharge flows out as a buoyant layer over heavier coastal water (Garvine and Monk 1974). In coastal areas with strong tidal currents, the outflow plume may be swept back into the estuary by the flood currents, forming a tidal-intrusion front (Simpson and Nunes 1981). In estuaries where tidal mixing is sufficient to inhibit development of persistent stratification, vertical and lateral shear in flood current may interact with the longitudinal-density gradient to produce relatively heavy water in the central part of the channel. The associated pressure field could drive a transverse two-cell circulation to form an axial convergence front (Nunes and Simpson 1985; Turrell and Simpson 1988). Frontal structures could also be produced during ebb flow, when relatively fast channel currents bring fresher upriver water alongside slower, saltier water over the shallow flanks. This condition could cause shoreward surface flow and induce front formation along either side of the channel (Huzzey and Brubaker 1988).

Observations have shown that tidal intrusion fronts are often associated with strong horizontal current convergence and downwelling, which not only play an important role in material transport and retention of plankton larvae, but also play a role in the conversion of tidal kinetic energy to potential energy (Largier 1993). Fronts that impact on living resources have long been recognized (Klemas and Polis 1977; Byrne et al. 1987). It can be expected that their presence is important to circulation/stratification of the estuary as a whole. They should be regarded as potentially important phenomena and deserve further study.

Figure 1 is a schematic drawing of a fully formed frontal system. The motion of the front and the circulation within the light-water pool generate a convergence at the surface front line. Once formed, the light-water pool may propagate at speeds up to the appropriate internal-wave phase speed. The light-water pool is depleted by mixing as the front ages, and large meanders may develop. At the surface, the convergence at the front line can reach tens of centimeters per second (Kupferman et al. 1973; Ingram 1976; Sarabun 1980). This forms a powerful mechanism for the concentration of surface material at the front line, usually accompanied by foam line. The foam line have been shown to possess concentrations of heavy metals as much as three orders of magnitude greater than surrounding waters (Szekielda et al. 1972; Sick et al. 1978). In addition, the associated downwelling at the frontal interface becomes an important mechanism for the introduction of surface-borne materials into the water column. The fronts themselves form a barrier to lateral mixing, so the water masses on either side

of the front may have radically different chemical and biological characteristics, often resulting in a pronounced color difference.

In the present study, a vertical two-dimensional model was used to calculate the hydrodynamic conditions in the Tanshui River estuary system and acted as basic data for theoretical analysis. The calculating results were also validated with filed observation. A tidal Froude number, which is the natural form arising from the work of Stommel and Farmer (1952), is employed. Instantaneous values for this parameter, which, takes into account the existence of significant tidal currents in the lower layer, are calculated in order to characterize the evolution of the stratification. Additionally, data from the Tanshui River estuary are employed to verify how well gravity current theory is satisfied. By using these results an attempt is made to relate the degree of stratification with deviations from gravity current behaviour.

FROUDE NUMBER ANALYSIS

An interfacial Froude number is classically used as a good representation of the stability of stratification. The standard interfacial Froude number, F_i , arise either or from the maximum flow condition under stable stratification (Stommel and Framer 1952) or from the critical condition for the breaking of interfacial waves propagating against a flow of speed $u_1 + u_2$ (Keulegan 1966)

$$\frac{u_1^2}{gh_1} + \frac{u_2^2}{gh_2} = \frac{\rho_2 - \rho_1}{\rho_2} = \frac{\Delta\rho}{\rho_2} \quad (1)$$

where u_i , h_i , and ρ_i are the velocities, thicknesses and densities of the upper ($i=1$) and lower layer ($i=2$)

Neglecting the velocity of the lower layer gives

$$F_i = \frac{u_1}{\sqrt{g'h_1}}$$

where $g' = g\Delta\rho/\rho_2$. This number is sometimes modified by substituting u_1 by $u_{12} = u_1 - u_2$, the relative velocity between both layers, apparently in order to minimize the above-mentioned approximation (Dyer 1973), giving

$$F_i = \frac{u_{12}}{\sqrt{g'h_1}} \quad (2)$$

F_i has a critical value of one, above which mixing develops.

The omission of u_2 is particularly unreal for tidal estuaries and, even if a relative velocity is introduced, the depth of the lower layer is not taken into account. Hence, for tidal estuaries a more realistic can be obtained from equation (1) by considering the effect of u_2 . In this way a (interfacial) tidal Froude number, F_i is obtained (Armi 1986), given by

$$F_i = \left[\frac{u_1^2/h_1 + u_2^2/h_2}{g'} \right]^{1/2}$$

which also has a critical value of unity.

In practice, however, a perfect two-layer system does not usually exist due to the finite thickness of the interface and the critical value can be expected to change. Long (1955) used a Froude number similar to F_i and found a critical value of $1/\pi$ for extreme case of a flow with a linear density gradient. In this paper, the thickness of interface has been included the lower layer. This is done for the sake of consistency with gravity current calculations, as explained below.

Fischer (1972) defined an estuarine Richardson number, Ri_e , which relates the input of buoyancy due to river flow to tidal velocities. An overall estuarine Froude number, F_e , can be obtained by taking the square root of the inverse Ri_e ; this gives

$$F_e = \left[\frac{u_{2,rms}^3}{g' u_f d} \right]^{1/2} \quad (4)$$

where u_f is the freshwater velocity at low water, given by $u_f = Q_f/A$, in which

Q_f is the freshwater discharge at low water and A is the area of the cross-section at the point considered; $u_{2,rms}$ is the root mean square tidal velocity, d is the total depth at the observation point and all the other parameters correspond to the low water situation. Fischer (1976) indicates that the transition between stratified and well-mixed estuaries occurs in the range $0.8 > Ri_e > 0.08$, which corresponds to $1.1 < F_e < 3.5$.

GRAVITY CURRENT THEORY

A gravity or density current consists of a wedge of fluid advancing into a surrounding liquid which has a different density (Figure 2). Benjamin (1968) studied the problem from a system of reference moving with the current and considered a flow force balance (momentum flux plus pressure force) between the approaching and receding parts of the stream, allowing for energy losses at the head. He showed that energy is conserved only if the thickness of the receding flow, h_2 , is half the total depth, d , and that a flow with energy losses is only possible, without external energy supply, if $h_1 < d/2$.

The velocity for the approaching stream, c , can be expressed as

$$c = C \sqrt{g' h_1} \quad (5)$$

where

$$C = \left[\frac{(1-\delta)(2-\delta)}{(1+\delta)} \right]^{1/2} \quad (6)$$

$d = h_1/d$ and $g' = g(\rho_2 - \rho_1)/\rho_2$, with ρ_1 the density of the advancing gravity current, ρ_2 the density of the surrounding fluid and h_1 the thickness of the gravity current. Equation (5) can be rewritten as

$$\frac{c}{(g'd)^{1/2}} = \left[\frac{(1-\delta)(2-\delta)\delta}{(1+\delta)} \right]^{1/2} \quad (7)$$

which, when differentiated with respect to δ , gives a maximum value of

$$c_{\max} = 0.5273(g'd)^{1/2} \quad (8)$$

corresponding to $h_1 = 0.3473d$. Values for the receding stream velocity, c_2 , can be related to c by a simple continuity argument

$$cd = c_2h_2 \quad (9)$$

A restriction in Benjamin's theory is that fluids are treated as inviscid. Hence, his theory does not allow for mixing between both fluids and neglects energy losses due to friction above the gravity current (or below if propagation is along the sea bottom) and interfacial friction. Furthermore, it assumes a constant depth (rigid lid), which is not necessarily true if the gravity current propagates along the air-sea interface.

The notation employed differs from Benjamin's original notation. In this way the approaching stream is easily identified with the seaward side of the front, while the receding stream corresponds to the lower layer in the stratified side of the frontal system. In Benjamin's theory, the velocities inside the gravity current (upper layer) are not considered. Hence, any possible relation between them, the motion of the gravity current and the degree of mixing at the interface between both fluids is discarded.

HYDRODYNAMIC MODEL

The Tanshui River is formed by the confluence of Tahan Stream, Hsintein Stream and Keelung River (Figure 3). The downstream portion of all three tributaries are influenced by tide, and subjected to sea water intrusion. Together, they formed the largest estuarine system in Taiwan, with its drainage basin including the capital city of Taipei. The major portion of the estuary system, upstream of Kuan-Du (Figure 3), lies within the Taipei basin, while the stretch downstream is confined by high mountains on both sides. In addition, the river is narrow that there is no significant wind-induced current in the river. The major forcing mechanisms of the flows are astronomical tide at river mouth and river discharges at upriver ends. Semi-diurnal tides are the principal tidal constituents, with a mean tidal range of 2.22 m and a spring tidal range of 3.1 m. The average river discharges are $62.1 \text{ m}^3/\text{s}$, $72.7 \text{ m}^3/\text{s}$, $26.1 \text{ m}^3/\text{s}$, respectively, in the Tahan Stream, Hsintein Stream and Keelung River. In addition to

the barotropic flows forced by tide and river discharges, the baroclinic flow forced by sea water intrusion is another important transport mechanism in the Tanshui River estuary system.

A laterally averaged two-dimensional model was applied to the Tanshui River estuary system. The model includes a feature of simulating shallow shoals or embayments as side storage areas, connecting to the main channel. The model solves the continuity, momentum and mass-balance equations with a finite difference scheme. The model has been applied successfully to the tributary estuaries of the Chesapeake Bay in the United States (Park and Kuo 1994, 1996). The model was expanded to include the capability to simulate tributaries as well as main stem estuary (Hsu et al. 1996, 1997, 1999). In applying to the Tanshui River system, the model treats the Tanshui River and Tahan Stream as the main stem and Hsintien Stream and Keelung River as tributaries. They are divided into 33, 14, and 37 segments, respectively, with a uniform segment length of 1.0 km. The vertical grid spacing is 1 m for all layers, except the surface layer which is variable, with 2 m at mean sea level. Details of model calibration and verification have been presented in Hsu et al. (1996, 1997, 1999).

A harmonic tide of eight constituents at the river mouth was used to force the model. The eight constituents are M_2 (12.42 h), S_2 (12 h), N_2 (12.9 h), K_1 (23.92 h), O_1 (25.82 h), K_2 (11.97 h), P_1 (24.07 h), and M_4 (6.2 h). The model simulation was conducted using the Q_{75} flow condition (Q_{75} is the annually flow that is equaled or exceeded 75% of time). Q_{75} discharges at the tidal upstream limits of the thanes major tributaries are $8.15 \text{ m}^3/\text{s}$, $20.2 \text{ m}^3/\text{s}$ and $3.61 \text{ m}^3/\text{s}$ for Tahan Stream, Hsintien Stream, and Keelung River, respectively. The 25 ppt salinity at the Tanshui River mouth was for boundary condition. The model was run for one-year (705 tidal cycles).

Figure 4 presents the model results during high and low tides in the Tanshui River-Tahan stream. Salinity shows a strong periodic fluctuation in response to tide, with high stratification at low tide and nearly well-mixed at high tide. Figure 5 presents the relationship between tidal amplitude, tidal currents and salinity in the estuary. If the estuary is of the correct depth and length then it is possible for tidal wave to enter, be reflected from the upstream and return in a time equal to a harmonic of the tidal period. The reflecting wave will then interface with the wave just entering. A standing wave system can thus be set up in the estuary. High and low waters and the time of turn of the current are simultaneous throughout the estuary. The tidal amplitude and salinity variation are thus 90° out of phase with current velocity.

THEORY APPLICATION

Instantaneous values of modeling result for the interfacial and Froude number,

F_i and F_r , was used to calculate at the stationary location for the estuary. The field data in the stratified side of the front has been approximated to that for a two-layer system by vertically averaging the salinity and velocity values over each layer, with the thickness of the interface included as part of the lower layer. Figure 6 presents the time series variation of $g' \left(= g \frac{\sigma\rho}{\rho_2} \right)$. It shows that g' is higher at low water than that at high water, thus the more stratification exists at low water and well-mixed occurs at high water. Figure 7 shows the temporal variation of F_i and F_r in the estuary. Both Froude numbers have similar patterns. Values of $F_i < 1.0$ correspond to well-stratified conditions. Values between one and as large as about three appear associated with conditions prior to quick mixing, while larger values correspond to well-mixed situations. During low water, values of $F_i < 3$ are located between stratification and well-mixed conditions. The modeling data shows the rupture of the front and the development of well-mixed conditions during high water. Figure 8 presents the temporal variation of F_r in the estuary. The F_r values obtained for the date under consideration and less than 1 that corresponds to stratification condition at low water. The F_r values are up to 10 that correspond to well-mixed condition at high water, and agree with Fischer's (1976) criteria.

For the estuary the continuous data taken from modeling results can be employed to make a check of gravity current behaviour using the data, values for c can be calculated either from equation 9 ($c = c_2 h_2 / d$) or from equations 5 and 6. In the first instance it will be called the 'observed' value because it arises from a simple continuity argument, while in the second it will be called the 'expected' or 'predicted' value because it comes from the use of gravity current theory. Figure 9 presents the check values for gravity current theory obtained in the estuary. It shows that predicted c is larger than observed c during low water, while predicted c is smaller than observed c during high water. From figure 9 three stages, indicated over the figure, may be distinguished: (1) near low water, the front is outside the estuary-the frontal system does not reach the observation point, the situation there resembling a one-layer flow down-estuary; (2) when the front approaches the observation point, a two-layer flow structure is formed, with relative up-estuary velocity in the lower layer, and (3) after the rupture of the front, a one-layer flow up-estuary takes place, the velocities considerably increasing. In the figure 9 also reveals that maximum velocity calculated from equation 8 approaches to predicted c .

Figure 10 presents the relative difference between the observed and predicted values (predicted minus observed divided by predicted value), $\Delta c/c$, plotted against the tidal Froude number. It can be anticipated that large positive values (c predicted larger than c observed) will be close to one-layer flux downstream situation, while

large negative values (the predicted value smaller than the observed one) will correspond to an approximate one-layer flow upstream situation. It is expected that value close to zero will correspond to a well-stratified two-layer flow, not too far from the front. From the data shown it is clear that the estuary corresponded to a distinct situation in which considerable stratification and good gravity current behaviour are present.

The Tanshui River estuary is a good example of a well-stratified estuary. The estuary develops well-mixed conditions during the flood, characterized by high Froude numbers. The front always breaks before the time of maximum flood velocities, usually occurring when the front is pushed up-estuary to a wider portion of the basin, while the upper layer has more difficulty in sustaining an adequate flow force balance; after this the tidal velocities are no longer restrained, usually showing a sudden increase.

It is worth mentioning that the frontal systems which develop at the estuary show considerable three-dimensional structure, apparently associated to their bottom shape. Shen and Kuo (1999) used a three-dimensional hydrodynamic model to investigate an estuarine frontal system in the lower James River. The model results were confirmed with field observations and compared with theoretical analysis. It is evident that a more adequate application of gravity current theory would need to take into account the estuary bathymetry.

CONCLUSION

Instantaneous values of the tidal Froude number, F_t , has been to reflect adequately the evolution of the stratification in the estuary considered. The calculations show that the classical criteria of mixing developing for $F_t > 1$ is essentially correct. Stratification may persist with value as high as 3, but corresponds to an unstable situation, previous to quick mixing.

Variations in the frontal relative velocity are probably associated to changes in the tidal velocities and the time delay of the upper layer to adjust to the flow force balance required by gravity current theory. When the upper layer is unable to approximately sustain this balance, either because the tidal velocities become too large or the front is moved up-estuary to much wider section of the basin, it is expected that the frontal system will break and part of the estuary will become mixed. Well-stratified estuaries, with approximate gravity current behaviour, may be expected in basins having relatively small tidal input, large river discharge and considerable depths.

ACKNOWLEDGMENTS

The study is supported by National Science Council, Taiwan, ROC, under grant

REFERENCES

1. Armi, L., "The hydraulics of two flowing layers with different densities," *Journal of Fluid Mechanics*, 163, 27-58, 1986.
2. Benjamin, T. B., "Gravity currents and related phenomena," *Journal of Fluid Mechanics*, 31, 209-248, 1968.
3. Byrne, R. J., et al., "Newport Island: An evaluation of potential impacts on marine resources of the lower James River and Hampton Roads," *Spec. Rep. in Appl. Marine Sci. and Oc. Engrg.*, No. 283, College of William and Mary, Virginia Institute of Marine Science, Gloucester Point, Va., 1987.
4. Dyer, K. R., "Estuaries: a physical introduction," Wiley, London, 1973.
5. Fisher, H. B., "Mass transport in partially stratified estuaries," *Journal of Fluid Mechanics*, 544, 671-687, 1972.
6. Fisher, H. B., "Mixing and dispersion in estuaries," *Annual Review of Fluid Mechanics*, 8, 107-133, 1976.
7. Garvine, R. W. and Monk, J. D., "Frontal structure of a river plume," *Journal of Geophysical Research*, 79, 2251-2259, 1974.
8. Huzzey, L. M. and Brubaker, J. M., "The formation of longitudinal fronts in a coastal plain estuary," *Journal Geophysical Research*, 93(C2), 1329-1334, 1988.
9. Hsu, M. H., Kuo, A. Y., Kuo, J. T. and Liu, W. C., "Study of tidal characteristics, estuarine circulation and salinity distribution in Tanshui River system (1)," *Tech. Rep. No. 239*, Hydrotech Research Institute, National Taiwan University, Taipei, Taiwan, 1996 (in Chinese).
10. Hsu, M. H., Kuo, A. Y., Kuo, J. T. and Liu, W. C., "Study of tidal characteristics, estuarine circulation and salinity distribution in Tanshui River system (2)," *Tech. Rep. No. 273*, Hydrotech Research Institute, National Taiwan University, Taipei, Taiwan, 1997 (in Chinese).
11. Hsu, M. H., Kuo, A. Y., Kuo, J. T. and Liu, W. C., "Procedure to calibrate and verify numerical models of estuarine hydrodynamics," *Journal of Hydraulic Engineering, ASCE*, 125(2), 166-182, 1999.
12. Ingram, R. G., "Characteristics of a tide-induced estuarine front," *Journal of Geophysical Research*, 86, 2017-2023, 1976.
13. Keulegan, G. H., "The arrested saline wedge," *In Estuary and Coastline*

- Hydrodynamics* (Ippen, A. T., ed.), McGraw-Hill, New York, 546-574, 1966.
14. Klemas, V. and Polis, D. F., "A study of density fronts and their effects on coastal pollutants," *Remote Sensing*, 6, 95-126, 1977.
 15. Kupferman, S. L., Klemas, V., Polis, D. F. and Szekiolda, K. H., "Dynamics of aquatic frontal systems in Delaware Bay," *EOS*, 54, 302, 1973.
 16. Long, R. R., "Some aspects of the flow of stratified fluids. III. Continuous density gradients," *Tellus*, 7, 342-357, 1955.
 17. Lagier, J. L., "Estuarine fronts: How important are they?," *Estuaries*, 16(1), 1-11, 1993.
 18. Nunes, R. A. and Simpson, J. H., "Axial convergence in a well-mixed estuary," *Estuarine Coastal and Shelf Science*, 20(5), 637-649, 1985.
 19. Park, K. and Kuo, A. Y., "Numerical modeling of advective and diffusive transport in the Rappahannock estuary, Virginia" *Estuarine and Coastal Modeling III: Proc., 3rd Int. Conf. In Estuarine and Coastal Modeling*, M. L. Spaulding et al., eds., ASCE, Reston, Va., 461-474, 1994.
 20. Park, K. and Kuo, A. Y., "A numerical model study of hypoxia in the tidal Rappahannock River of Chesapeake Bay," *Estuarine, Coastal and Shelf Science*, 42(5), 563-581, 1996.
 21. Stommel, H. and Farmer, H. G., "Abrupt change in width in two layer open channel flow," *Journal of Marine Research*, 11, 205-214, 1952.
 22. Sarabun, C. C., "Structure and formation of Delaware Bay fronts," *Ph. D dissertation, University of Delaware*, Newark, Del., 1980.
 23. Shen, J. and Kuo, A. Y., "Numerical investigation of an estuarine frontal and its associated eddy," *Journal of Waterway, Port, Coastal, and Ocean Engineering*, ASCE, 125(3), 127-135, 1999.
 24. Sick, L. V., Johnson, C. C. and Engel, A., "Trace metal enhancement in the biotic and abiotic components of an estuarine tidal front," *Journal of Geophysical Research*, 83, 4659-4667, 1978.
 25. Simpson, J. H. and Nunes, R. A., "The tidal intrusion fronts: An estuarine convergence zone," *Estuarine, Coastal and Shelf Science*, 13, 257-266, 1981.
 26. Szekiolda, K. H., Kupferman, S. L., Klemas, V. and Polis, D. F., "Element enrichment in organic films and foam associated with aquatic frontal systems," *Journal of Geophysical Research*, 77, 5278-5282, 1972.
 27. Turrell, W. R. and Simpson, J. H., "The measurement and modelling of axial

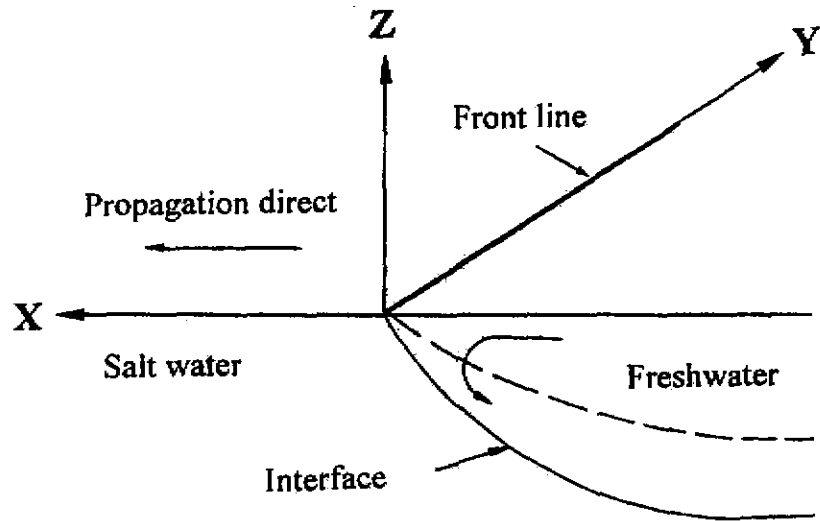


Figure 1 Schematic diagram of a fully developed estuarine front.

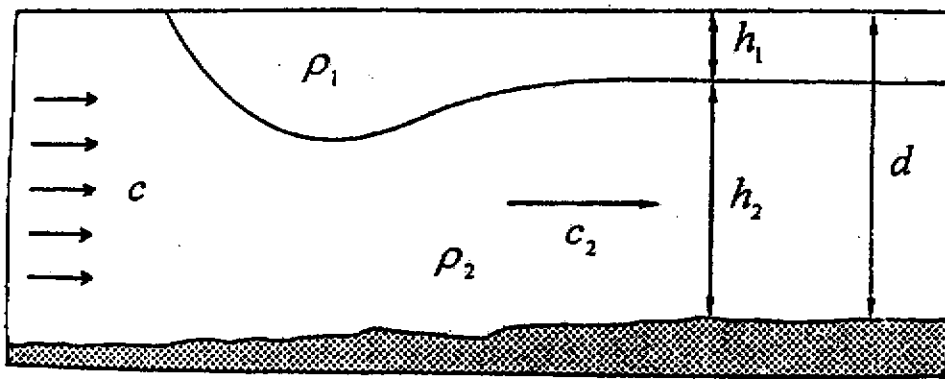


Figure 2 Scheme to show the progression of gravity current along the water surface.

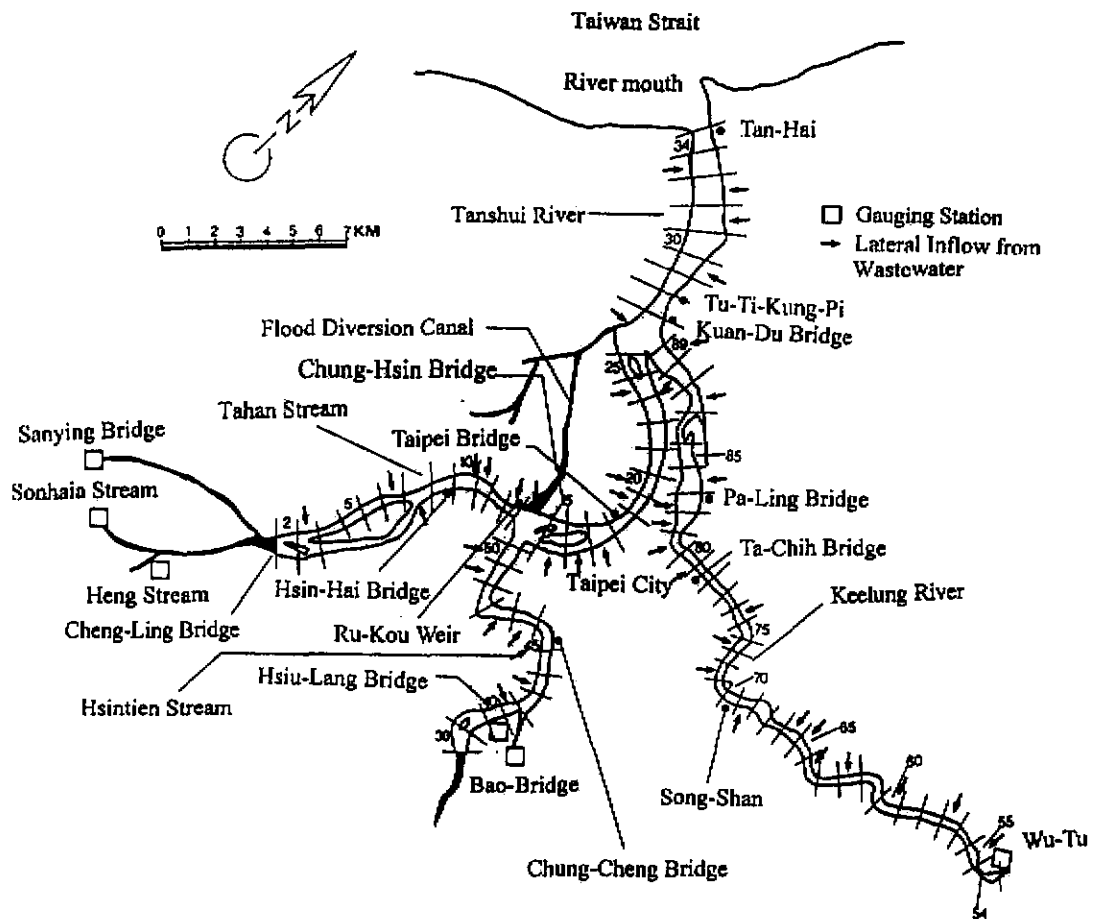


Figure 3 Map of the Tanshui River estuarine system and the model segment (Kuan-Du is observational station of the tidal front).

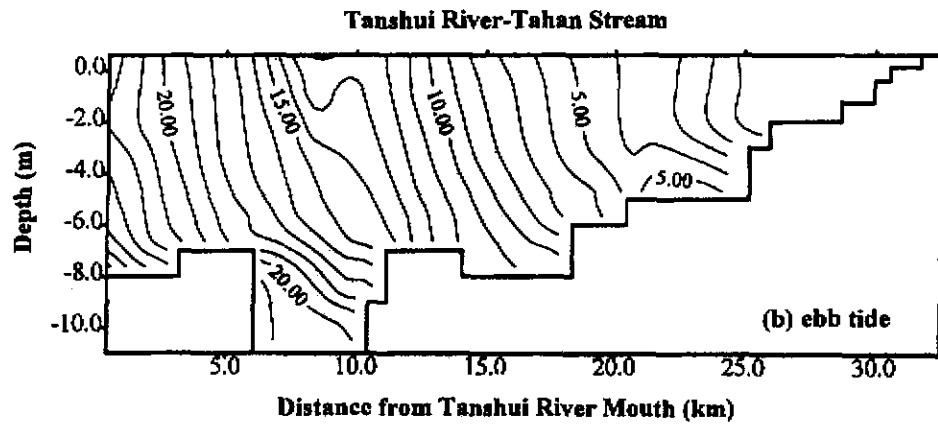
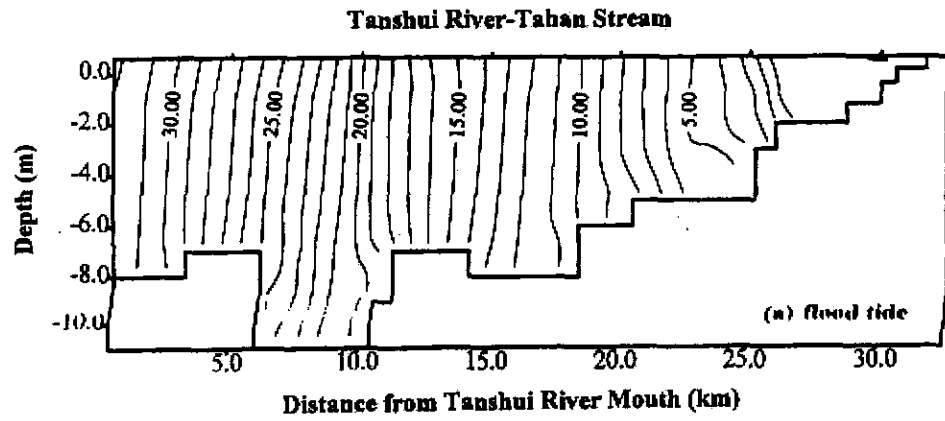


Figure 4 Computed salinity distributions in the Tanshui River-Tahan Stream
 (Numbers on the contours refer to the salinity in parts per thousand).

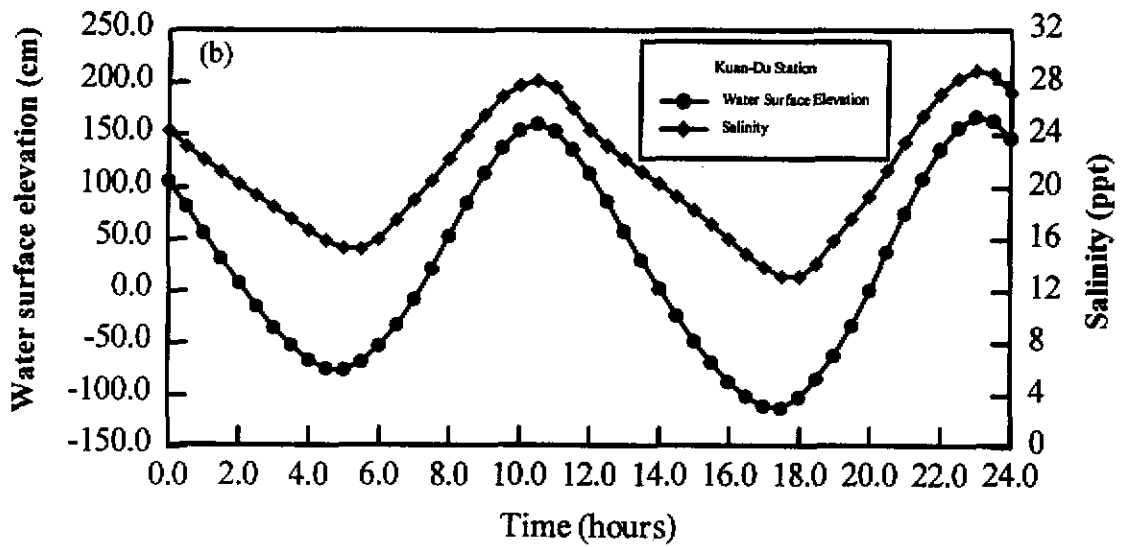
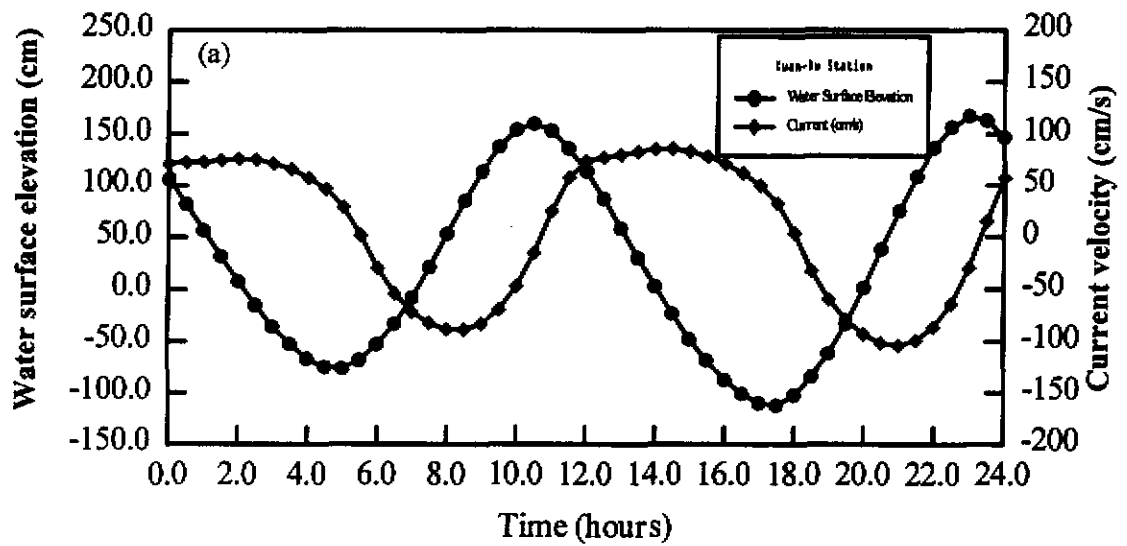


Figure 5 Temporal variations of water surface elevation, current and salinity at Kuan-Du station (a) water surface elevation and current (b) water surface elevation and salinity.

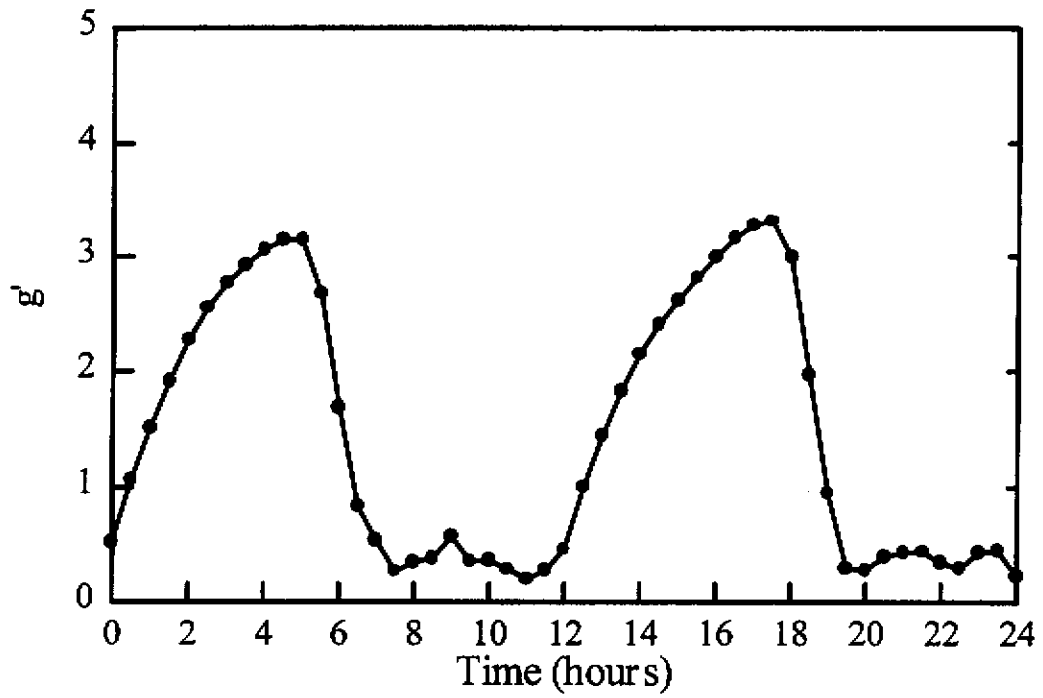


Figure 6 Temporal variation of $g' (= g \frac{\Delta\rho}{\rho_2})$.

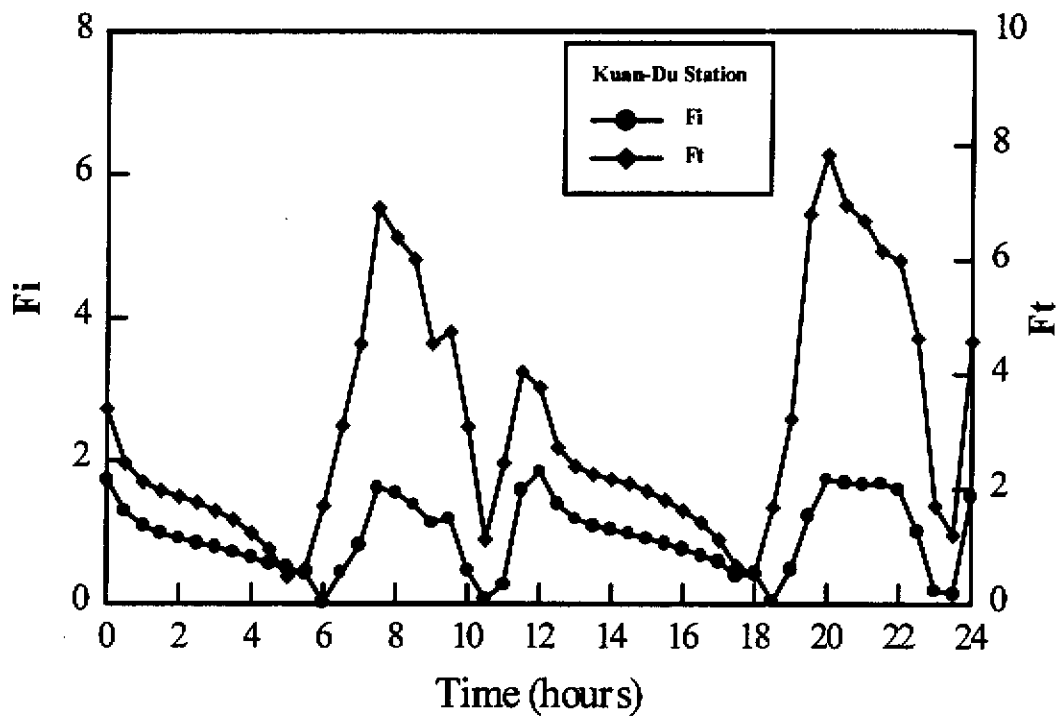


Figure 7 Temporal variation of tidal Froude number at Kuan-Du station.

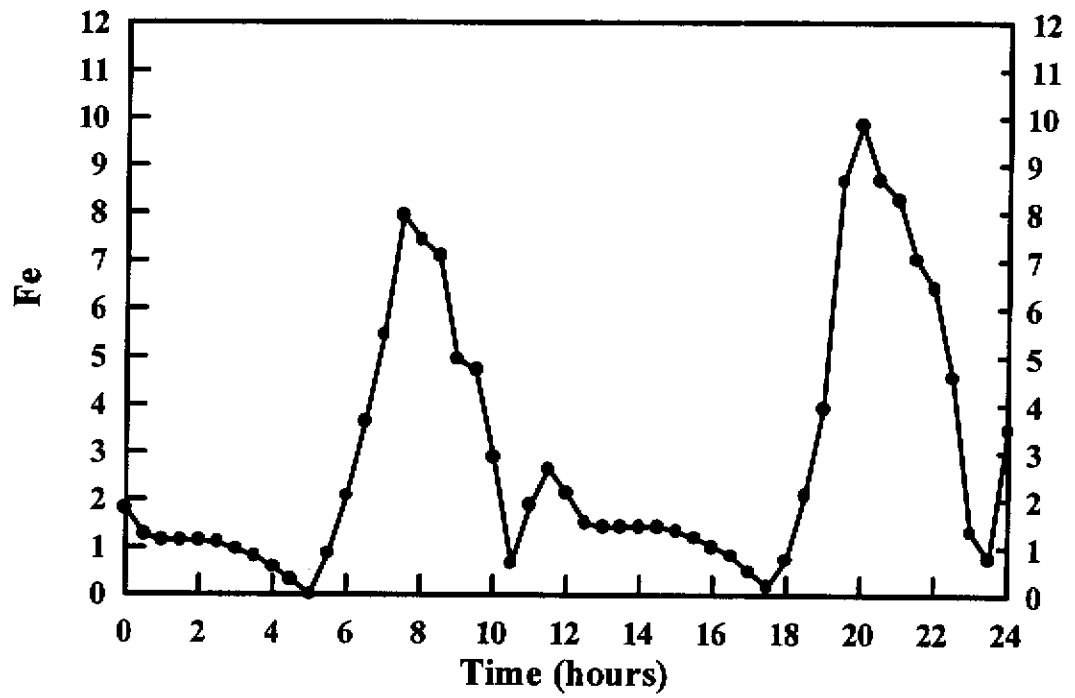


Figure 8 Temporal variation of estuarine Froude number at Kuan-Du station.

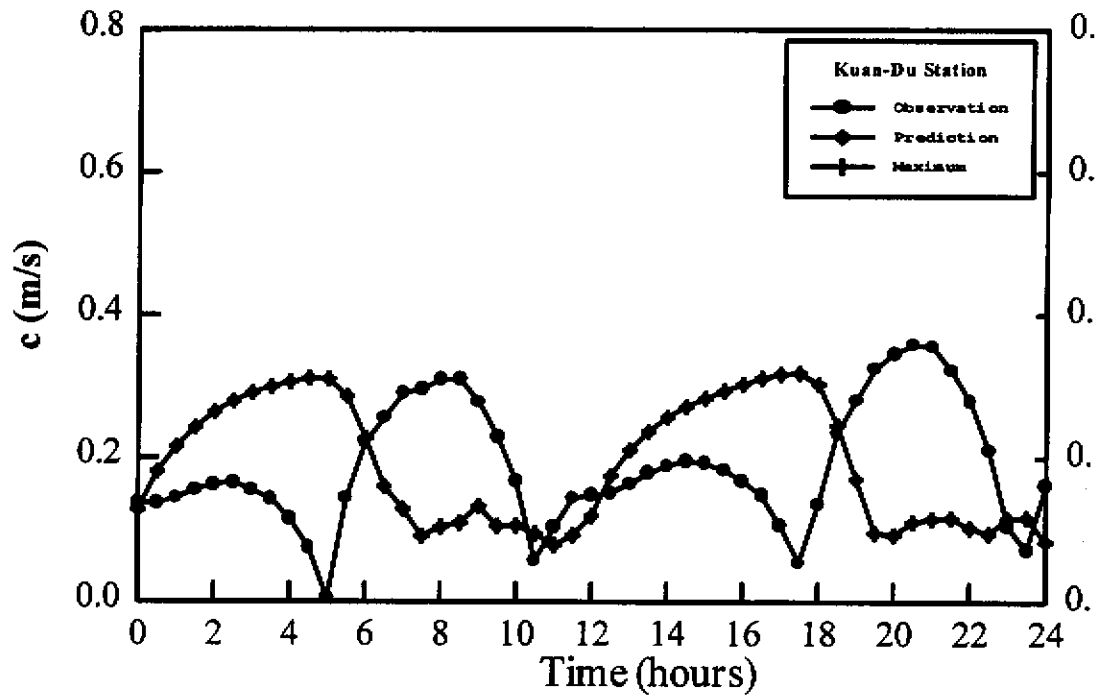


Figure 9 Gravity current behaviour at Kuan-Du station.

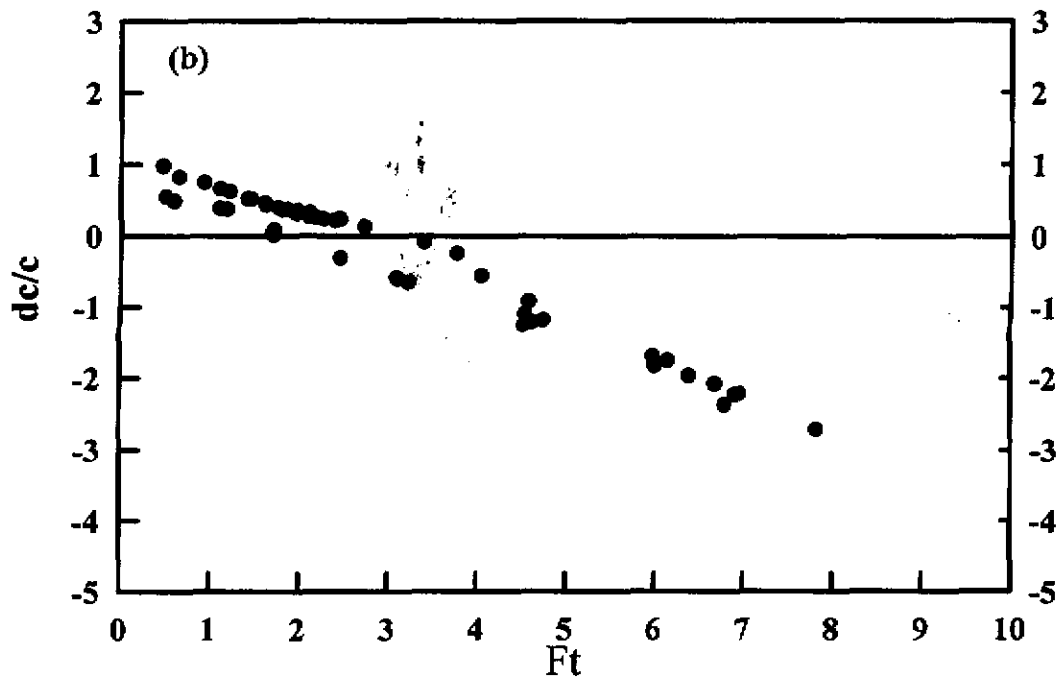
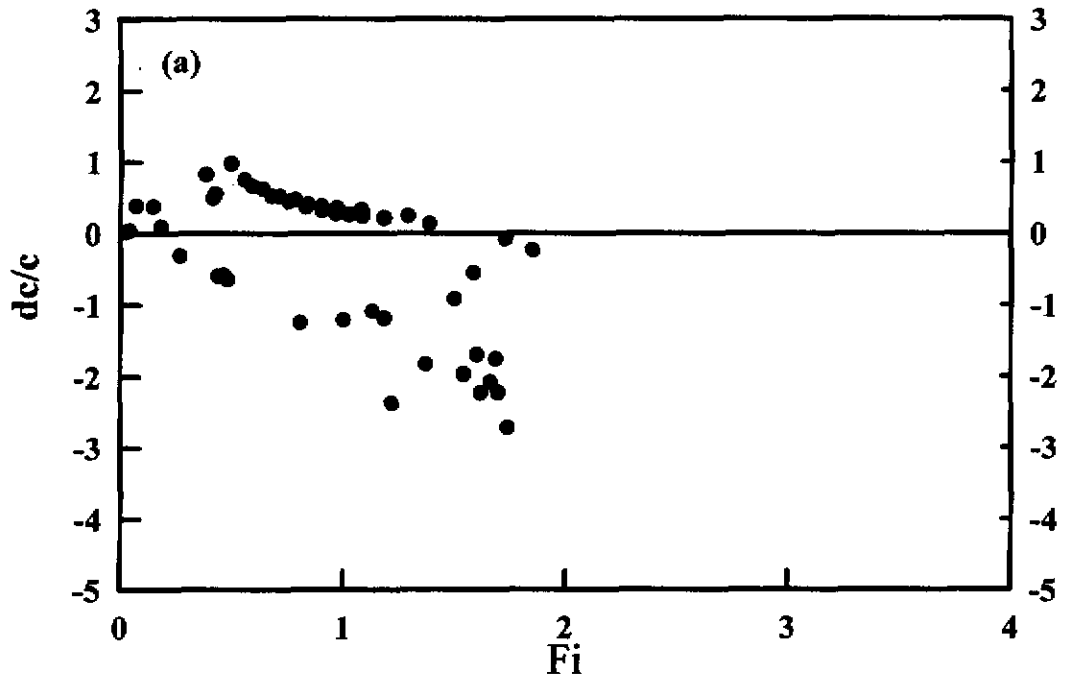


Figure 10 Deviations from gravity current behaviour versus
 (a) interfacial Froude number (b) tidal Froude number.



**Pacific
Institute**
for the Mathematical Sciences

Department of Mathematical Sciences
Faculty of Science
501 Central Academic Building
University of Alberta
Edmonton, Canada T6G 2G1

Phone: (780) 492-4308
Fax: (780) 492-6826
E-mail: pims-ua@math.ualberta.ca

February 26, 2001

Dear Ming-Hsi Hsu,

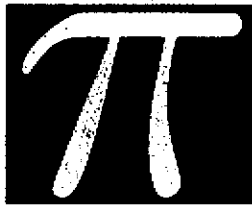
We are pleased to inform you that your paper "Investigation of the Tidal Intrusion Front in Estuary" has been accepted for oral presentation at Wave Phenomena III: Waves in Fluids from the Microscopic to the Planetary Scale to be held June 11-15, 2001 at Edmonton Alberta, Canada. Your presentation is to be of 20 minutes duration including time for questions. Please let us know well in advance of any special audio-visual needs apart from overheads. Registration can be completed on the Web at <http://www.gemsregistration.com/events/waves/index.html>. You are responsible for arranging your own accommodation. You can find all the necessary information at <http://waves3.math.ualberta.ca/index.html#accommodation>. If you require a letter for immigration, please send a request via email to mbareil@ualberta.ca.

Looking forward to seeing you at Waves III.

A handwritten signature in black ink, appearing to read 'Bryant Moodie'.

The Organizers, Waves III

T. Bryant Moodie
Andrew Bush



The
**Pacific
Institute**
for the Mathematical Sciences

Department of Mathematical Sciences
Faculty of Science
501 Central Academic Building
University of Alberta
Edmonton, Canada T6G 2G1

Phone: (780) 492-4308
Fax: (780) 492-6826
E-mail: pims-ua@math.ualberta.ca

February 26, 2001

Dr. Ming-Hsi Hsu
Hydrotech Research Institute
National Taiwan University
No. 158 Chow-Shan R
Taipei 10617
Taiwan

Dear Dr. Ming-Hsi Hsu,

Thank you for accepting our invitation to visit the Department of Mathematical Sciences from June 11 to June 15, 2001 as a participant for the Wave Phenomena III: Waves in Fluids from the Microscopic to the Planetary Scale.

You will be acting as a participant in the Wave Phenomena III: Waves in Fluids from the Microscopic to the Planetary Scale conference.

You will be responsible for all your expenses (conference fees, travel and accommodations).

Bona fide Guest Speakers are permitted to enter Canada directly as visitors and do not require an Employment Authorization as per R19(1)(o) of the Immigration Manual. However, citizens from some countries (specified in the immigration Act) must obtain visitor's visas prior to entering Canada. If you are from such a country, please ensure that you apply for a visa, prior to entering Canada, through a Canadian Visa Post. If you are uncertain as to visa requirements from your country, you are urged to check with the nearest Canadian Consulate/Embassy concerning the current regulations.

If you do not require a visa, please carry this letter with you when you arrive and show it to the admitting Customs/Immigration Officer at port-of-entry **whether or not you are asked for it.**

(.../2)

If you are a citizen or permanent resident of a country other than the United States, St. Pierre and Miquelon, or Greenland, you must be in possession of a valid passport upon arrival. This applies also to citizens from other countries who are entering Canada via the United States and to those who have been temporary residents in the United States without having acquired permanent resident status.

Citizens and permanent residents of the United States may visit Canada without a passport but should carry evidence of their status, such as a birth certificate or naturalization papers. (A driver's license does not constitute such evidence.)

Please inform us of the name of the carrier, flight number, port-of-entry, and the date and time of your arrival so that we may notify Canada Immigration authorities at port-of-entry in advance of, and make them aware of the reason for, your visit.

Yours sincerely,

A handwritten signature in black ink, appearing to read 'T. Moodie', with a long horizontal flourish extending to the right.

Dr. T. Bryant Moodie
Professor of
Mathematical Sciences &
Site Director of
The Pacific Institute for the Mathematical Sciences

cc: Gail S. Bamber
Coordinator, Immigration & Advertising